

Comparison of Diameters of Disk Microelectrodes Obtained from Microscopes with Those Evaluated from Steady-State Currents

Koichi Aoki*, Chun Ouyang, Chaofu Zhang, Jingyuan Chen, Toyohiko Nishiumi

Department of Applied Physics, University of Fukui, 3-9-1 Fukui, 910-0017 Japan

*E-mail: kaoki@u-fukui.ac.jp

Received: 5 March 2012 / Accepted: 28 May 2012 / Published: 1 July 2012

Diameters of disk microelectrodes evaluated from steady-state diffusion-controlled currents by use of Saito's equation were smaller than geometrical diameters obtained from a scanning electron microscope (SEM) when the diameters were less than 4 μm . The smallest electrode that could be compared had the diameters 0.007 μm by the current and 0.11 μm by the SEM. With a decrease in the electrode, the observed currents were smaller than those predicted from Saito's equation. As a reason of the blocking of diffusion, memory diffusion was taken into account. It includes a delay or a displacement of the diffusion flux in the Fick's first law. The equation for memory diffusion was solved for the hemispherical and the disk electrode to give expressions for the steady-state currents. The experimental results allowed us to determine the displacement, 0.9 μm , as a blocking parameter.

Keywords: diffusion-controlled current at microelectrodes; geometrical diameters; steady-state voltammetry; images by SEM; Saito's equation

1. INTRODUCTION

Geometry and diameter of a disk microelectrode more than 10 μm can be measured accurately with an optical microscope. When a diameter is less than 2 μm , an optical microscope fails to distinguish even the location of the electrode [1]. Then the diameter has been evaluated from the steady-state diffusion-controlled limiting current, I_L , of a redox species [2,10] by use of Saito's equation [11], $I_L = 4Fc^*Da$, where c^* is concentration of the redox species, D is the diffusion coefficient, and a is the radius of the electrode. Known values of c^* , D and I_L allow us to evaluate the radius a . Advantages of this technique are not only convenience of the determination of a but also provide high accuracy and sensitivity without exploitation of techniques of mounting microelectrodes

on an electron microscope. A disadvantage is a loss of information on electrode geometry such as a disk, an ellipse or indeterminate form with rough boundaries. However, it has been demonstrated that the radius evaluated is close to that of a perfect circle of which area is the same as that of deformed electrode [12]. Radii evaluated from voltammetric currents have been reported to be close to the geometric radii [3,5,13,18].

The theory of the steady-state current at a disk microelectrode mentions that the current density is infinite at the edge of the electrode [1,19,20]. Since the current density should be finite in reality, Saito's equation is likely to overestimate the total current. In order to respond to this question, we compared the diameter of disk electrodes determined by the currents with those by a scanning electron microscope (SEM) [1]. The diameters by both methods agreed when they were more than 10 μm . When diameters ranged from 1 to 4 μm , those by the currents from Saito's equation were smaller than those by SEM. The underestimation is opposite to effects of surface roughness [21,22]. It can be partly explained in terms of partially blocked electrodes [23,25], if electrode surfaces are coated.

A possible explanation of the underestimation is a limitation of the diffusion law, exemplified by memory diffusion in the Fick's first law [1]. The flux in memory diffusion is generated with a delay from the formation of concentration gradient. Consequently, currents are observed smaller than the conventional values. The parabolic differential equation with the memory effects was first introduced to problems of heat conduction [26-30] and then was applied to electrochemical subjects [31]. The memory effect is based on the empirical rule that a cause necessarily precedes an effect. The rule has been demonstrated to be valid for the precedence of the concentration gradient (a cause) over the diffusion flux (an effect) by Monte Carlo simulation [32].

We report here the comparison of diameters of disk electrodes by the two methods, focusing especially diameters less than 1 μm . Microelectrodes exhibiting reproducible voltammograms can be fabricated by embedding a thin platinum wire with glass and being polished. SEM images of the electrodes less than 1 μm exhibit generally vague boundaries between the electrode and glass. Errors involved in the SEM images are covered with a number of fabricated electrodes. We derive expressions for the diffusion-controlled current at a disk microelectrode with memory effect with the use of the model of sluggish charge transfer reaction.

2. EXPERIMENTAL

A key of fabricating microelectrodes was to use such a short glass tube that the electrode could be mounted in a sample holder of a SEM. Disk electrodes were fabricated through a series of the procedures: (i) making an electric contact of 0.03 mm platinum wire to a tungsten wire, (ii) etching electrochemically the Pt wire in CaCl_2 solution, (iii) shielding the wire with a glass tube by heat, and (iv) polishing it under ac-current monitoring [33]. The exposed Pt surface was observed with an optical microscope, VH-Z450 (Keyence, Osaka) and a SEM, S-2600H (Hitachi). An electric contact with the earth of the SEM instrument was made with carbon tape.

The potentiostat, HECS 972 (Huso, Kawasaki), was controlled with a home-made soft-ware. The reference electrode was Ag|AgCl (3 M (= mol dm⁻³) NaCl). Voltammetry was carried out in deaerated solution in a Faraday cage.

Ferrocene was purified by sublimation. Solutions used were 0.5 M tetrabutylammonium perchlorate in acetonitrile including ca. 1 mM ferrocene. Accurate concentrations of ferrocene were determined by the combinational use of voltammetric peak currents at the electrodes 1.6 mm and 0.1 mm in diameters [34]. This technique was composed of carrying out voltammetry at the two electrodes for the potential scan rates, ν , in the range from 10 to 100 mM s⁻¹, evaluating the proportionality constant of the peak current, I_p , vs. $\nu^{1/2}$ at the 1.6 mm electrode, evaluating the extrapolated limiting current, I_L , to $\nu^{1/2} \rightarrow 0$ at the 0.1 mm electrode, and taking the ratio of the $(I_p \nu^{-1/2})^2/I_L$.

3. THEORY OF STEADY-STATE CURRENT

3.1 Steady-state currents including delay of diffusion

Fick's first law mentions that a diffusion flux is caused simultaneously by gradient of concentration, c . The flux J in the x -direction is expressed by $J(t,x) = -D\partial c(t,x)/\partial x$, where D is the diffusion coefficient. Here the occurrence of the gradient is a cause, whereas the flux is an effect. According to the empirical rule that a cause necessarily precedes an effect, the flux should be delayed from the occurrence of the gradient. Therefore, a reasonable relation includes a delay of the flux by τ .

$$J(t + \tau, x) = -D\partial c(t, x) / \partial x \quad (1)$$

The expression same as Eq. (1) has already been obtained in the field of heat conduction [28-30]. Expressing Eq. (1) by the Taylor expansion and taking the first two terms, we have

$$J(t, x) + \tau \partial J(t, x) / \partial t = -D\partial c(t, x) / \partial x \quad (2)$$

When the flux is eliminated from Eq. (2) with the equation of continuum, $\partial c / \partial t = -\partial J / \partial x$, we obtain the Fick's second law with memory effects, $\partial c / \partial t + \tau (\partial^2 c / \partial t^2) = D(\partial^2 c / \partial x^2)$. Solutions of this equation with chronoamperometric conditions have been obtained [35] to exhibit the behavior similar to the delay by electrode kinetics. When the initial condition is a delta function for $c(x)$, the Laplace transformed solution has been derived in analytical form [1]. The average of the square distance by diffusion is expressed by[1]

$$\langle x^2 \rangle = 2D(t - \tau) \equiv 2Dt - \delta^2 \quad (3)$$

Here, $\delta = (2D\tau)^{1/2}$ is a diffusion distance caused by the delay, τ . The term, $\partial J/\partial t$, in Eq. (2) is rewritten as $(\partial J/\partial r)(\partial r/\partial t)$ for a distance r of the polar coordinate. Since $(\partial r/\partial t)$ at a short time and a short distance is close to δ/τ , the second term in Eq. (2) becomes approximately $\delta(\partial J/\partial r)$. Therefore, the Fick's first law with memory under the steady state is given by

$$J(r) - \frac{dJ(r)}{dr} \delta = -D \frac{dc(r)}{dr} \quad (4)$$

3.2 Hemi-spherical electrodes

The electrochemical reaction considered here is one-electron oxidation at the hemi-spherical electrode a in radius. The current is assumed to be controlled by hemi-spherical diffusion under the steady state. By letting r be the axial coordinate from the center of the sphere, the equation of continuum under the steady-state is expressed by $d(r^2J)/dr = 0$. This yields $J = Ar^{-2}$, where A is an integration constant. Inserting this relation into Eq. (4) and integrating dc/dr under the conditions of $c(a) = 0$, $c(\infty) = c^*$, we have $A = -c^*Da^2/(a+\delta)$. Then the flux is expressed by

$$J(a) = -c^*D/(a+\delta) \quad (5)$$

Since $J(a)/c^*$ stands for the transport velocity of the reduced species through the diffusion layer, the inverse,

$$-c^*/J(a) = a/D + \delta/D \quad (6)$$

means the time traversing the diffusion layer. The traversing time is a sum of the time (a/D) without the memory and the electrode-independent time δ/D . The simple sum of the times reminds us of similarity to a delay by the electrode kinetics, i.e. a sum of the diffusion time and the kinetic time.

In order to find the similarity to the electrode kinetics, we consider the irreversible oxidation with the one-electron oxidation when diffusion includes no memory effect. The flux which is controlled by the forward reaction rate constant, k_f , is given by

$$-J(a) = k_f c(a) \quad (7)$$

Inserting the solution of the equation of continuum, $J = Ar^{-2}$, into the Fick's first law, $J = -D(dc/dr)$, and integrating the resulting equation under the condition $c(\infty) = c^*$, we obtain $c(r) = c^* + A/Dr$. Inserting this equation $J = -D(dc/dr)$ and eliminating A , we obtain $c(r) = c^* + J(r)r/D$. Setting $r = a$ and eliminating $c(a)$ by use of Eq.(7) gives

$$-c^*/J(a) = a/D + 1/k_f \tag{8}$$

Comparison of Eq. (8) with Eq. (6) yields the equivalence, $k_f = D/\delta$, indicating a similarity of the memory-diffusion current to the partially charge transfer controlled current. The memory diffusion is discriminated against the electrode kinetics in the point that it has no potential dependence.

We denote the geometrical radius as a_{sem} , and the electrochemically evaluated radius as a_{cv} . The total current for the former is given by $2\pi a_{sem}^2 J(a_{sem}) = -c^* D a_{sem}^2 / (a_{sem} + \delta)$ through Eq. (5), whereas that for the latter is $-c^* D a_{cv}$ because of $\delta = 0$. Since the both fluxes are equal, we have $a_{sem}^2 / (a_{sem} + \delta) = a_{cv}$. The inverse form is given by

$$a_{sem} / a_{cv} = 1 + \delta / a_{sem} \tag{9}$$

This predicts that plot of a_{sem}/a_{cv} against $1/a_{sem}$ falls a line with an intercept with unity. The slope yields a value of δ .

3.3 Disk microelectrodes

We apply the replacement $k_f = D/\delta$ to the expression for the kinetic steady-state current at the disk microelectrode a in radius. The steady-state current, I , of the Butler-Volmer type at any potential, E , is given by 36

$$I / I_L = (1 + e^{-\zeta})^{-1} f_1 \tag{10}$$

Where

$$\begin{aligned} \lambda &= (a/D)(k_f + k_b) \\ \zeta &= (E - E_0')F / RT \end{aligned} \tag{11}$$

Here, k_b is the backward rate constant, and E_0' is the formal potential. The auxiliary variable, f_1 , for λ , satisfies the following equation at an extremely large integer N and integers k (from 1 to N)

$$4 \sum_{m=1, \neq k}^N \frac{(m - \frac{1}{2})(m - \frac{3}{2}) \cdots \frac{1}{2}}{(m-1)!(2m-2k+1)} f_m + (4k - 2 + \pi\lambda) \frac{(k - \frac{3}{2})(k - \frac{5}{2}) \cdots \frac{1}{2}}{(k-1)!} f_k = \frac{\pi\lambda}{2k-1} \tag{12}$$

Equation (12) is a simultaneous equation with f_k variables. Analytical expressions for f_1 at $N=1$ and 2 are given by respectively

$$\begin{aligned} (f_1)_{N=1} &= \pi\lambda / (\pi\lambda + 2) \\ (f_1)_{N=2} &= [(\pi\lambda + \frac{16}{3})\pi\lambda] / [(\pi\lambda)^2 + 8\pi\lambda + 16] \end{aligned}$$

The variable f_1 in Eq. (10) corresponds to $(f_1)_{N \rightarrow \infty}$. Curves of $(f_1)_N$ vs. λ were obtained for $N = 1, 2, \dots$ by solving N -simultaneous equation (12) by use of the Gauss-Jordan method until they were convergent. Values of $(f_1)_N$ were converged for $N > 50$ within 1 % errors.

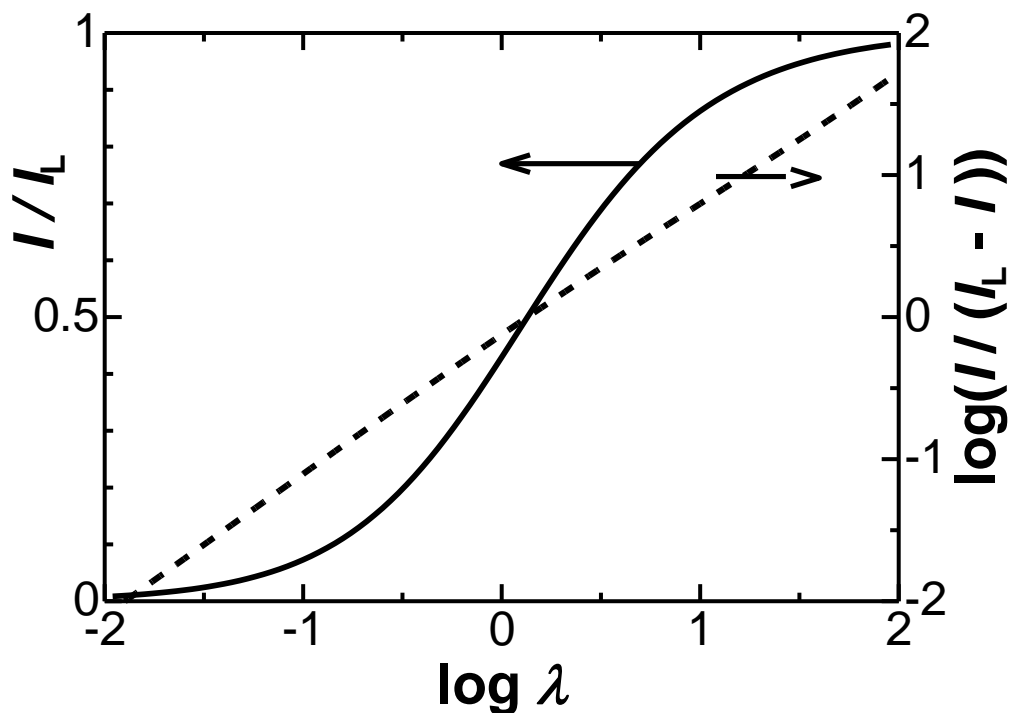


Figure 1. Variation of the normalized steady-state current complicated with electrode kinetics with the logarithm of the kinetic parameter, λ , obtained from Eq. (10) and (12). The dashed line is its logarithmic plot.

Figure 1 shows the variation of I/I_L with $\log \lambda$. Since $\log \lambda$ for $k_b = 0$ corresponds to the electrode potential, the curve in Fig.1 is equivalent to the current voltage curve. The plot of $\log(I/(I_L - I))$ against $\log \lambda$ falls on a line, represented empirically by

$$I/(I_L - I) = 0.702\lambda^{0.952} \tag{13}$$

When the forward and the backward rate constants are replaced by D/δ and zero, respectively, we obtain the expression for the diffusion-controlled limiting current with memory:

$$I = \frac{4Fc * Da_{sem}}{1 + 1.43(a_{sem} / \delta)^{0.952}} \tag{14}$$

On the other hand, the current for a_{cv} is defined by

$$I = 4Fc * Da_{cv} \tag{15}$$

Eliminating I from Eq. (14) and (15) yields

$$a_{\text{sem}}/a_{\text{cv}} - 1 = 1.43(\delta/a_{\text{sem}})^{0.952}$$

or

$$\log\left(\frac{a_{\text{sem}}}{a_{\text{cv}}} - 1\right) = 0.154 + 0.952 \log \delta - \log a_{\text{sem}} \quad (16)$$

Plot of $\log(a_{\text{sem}}/a_{\text{cv}} - 1)$ against $\log(a_{\text{sem}})$ should show a line with slope of -1. The intercept allows us to evaluate δ .

4. RESULTS AND DISCUSSION

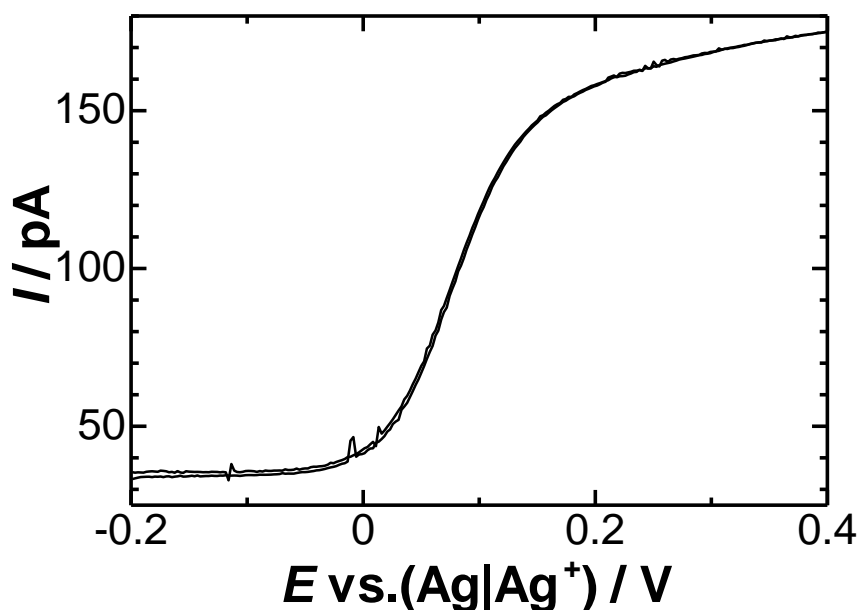


Figure 2. Cyclic voltammograms of 1.36 mM ferrocene in 0.5 M tetrabutylammonium perchlorate + acetonitrile at the glass-coated platinum electrode with $a_{\text{cv}} = 117$ nm for the scan rate, 10 mV s^{-1} .

Cyclic voltammetry of ferrocene in 0.5 M tetrabutylammonium perchlorate of acetonitrile solution was made at the fabricated disk microelectrodes, where concentrations of ferrocene were determined by the method of two electrodes. The voltammograms had little hysteresis, as is shown in Fig. 2. The difference of halfwave potentials of the forward and the backward waves were less than 7 mV. Voltammograms with halfwave potential differences over 15 mV were not used for the data analysis. They did not vary with iterative scans at least 10 times. The limiting currents were invariant to scan rates less than 50 mV s^{-1} . Currents, $I(E)$, at potentials E less than the limiting current domain

were plotted in the form of $\log[I(E)/(I_L - I(E))]$ vs. E for $0.05 < I/I_L < 0.95$. They fell on a line, the inverse slope of which was (61 ± 3) mV. This fact suggests one-electron reversible oxidation.

We evaluated the diffusion coefficient of ferrocene in acetonitrile from the proportional constant of the peak current at the electrode 1.6 mm in diameter to $v^{1/2}$ for a known concentration of ferrocene. We obtained $D = 2.00 \times 10^{-5} \text{ cm}^2 \text{ s}^{-1}$. Values of a_{cv} were determined by Eq. (15) (Saito' equation) with the help of known values of c^* and D . Figure 3 shows variation of the halfwave potentials, $E_{1/2}$, with logarithm of the radii. The independence of halfwave potentials from the radii indicates that the current-potential curves should obey the Nernst equation even at the smallest electrode, $a_{cv} = 3$ nm.

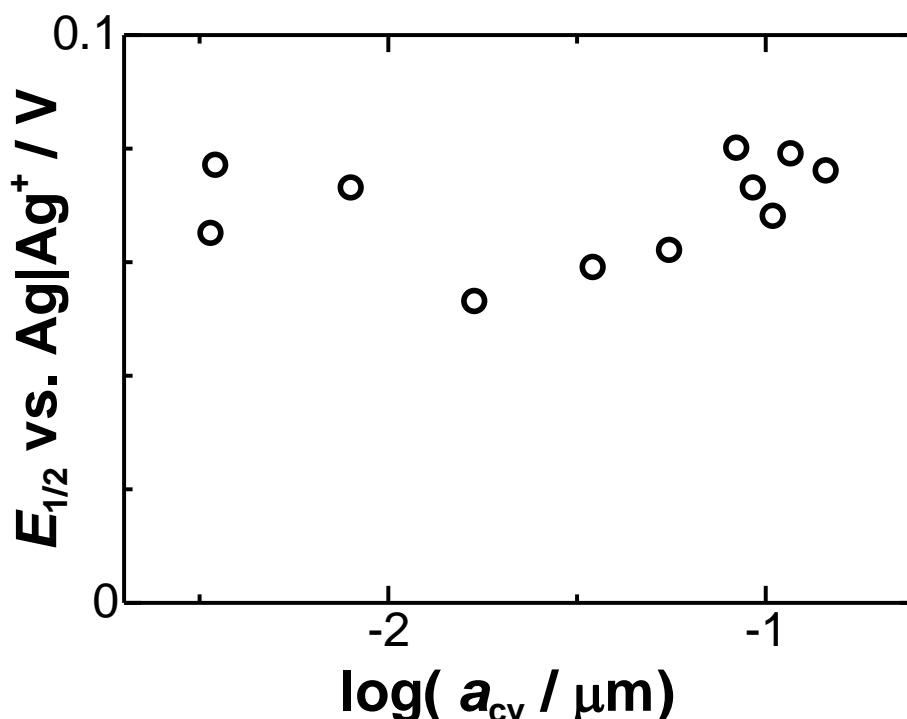


Figure 3. Variation of the halfwave potentials with logarithms of the radii, determined by the limiting currents through Saito's equation.

The electrode was mounted on the optical microscope in order to search a location of Pt on the glass surface. The surface of Pt looked a bright dot, depending on directions of incident light. This direction-depending reflection light was an identification of the Pt surface against the glass surface. In contrast, a SEM image had a black domain surrounded with the glass (white), at the center of which a gray spot could be seen, as shown in Fig. 4. Comparing the geometry and the diameter of the gray spot with the image by the optical microscope, we identified the gray spot as the exposed platinum. Since the polished surface is composed of only two domains of glass and platinum, the appearance of the three (white, black and gray) domains seems to be unreasonable. We confirmed from SEM images of a boundary between glass and platinum of a large electrode that the black domain always appeared around the boundary on the glass side.

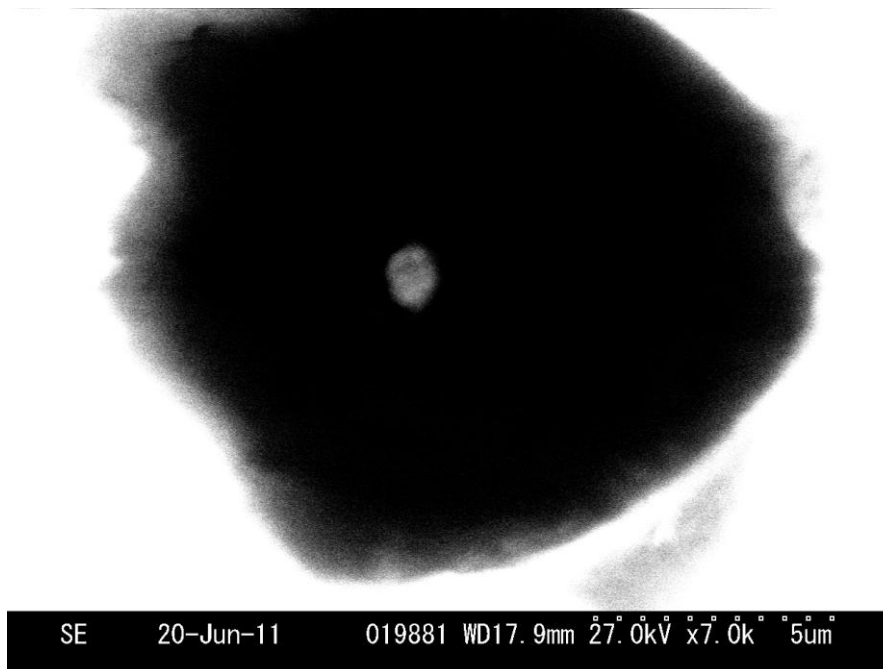


Figure 4. Photograph of SEM of the glass-coated platinum electrode ca. 0.7 μm in diameter, which was found at the center of the black domain as a gray spot.

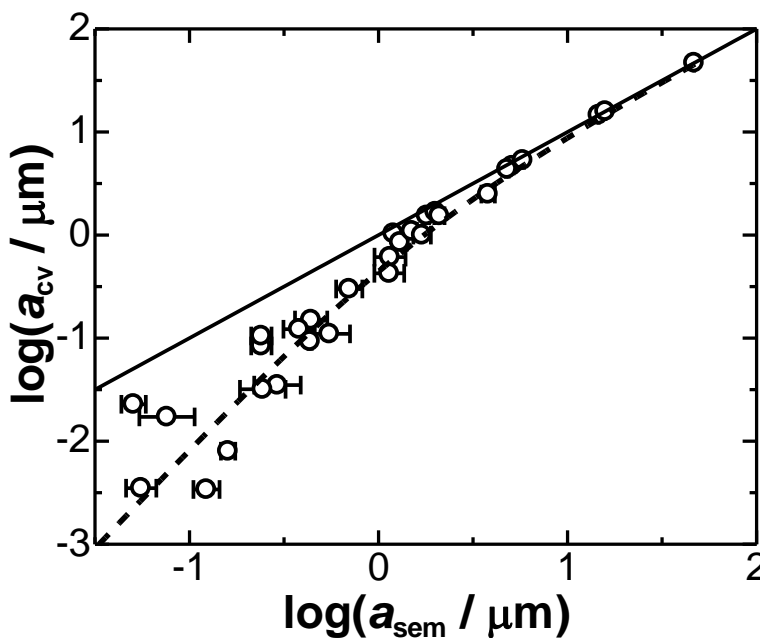


Figure 5. Logarithmic plots of the radii evaluated from CV and SEM. The solid line is for $a_{cv} = a_{sem}$. The dashed curve was obtained from Eq. (16) for $\delta = 0.88 \mu m$.

The concept of observing the three domains has been described on the basis of the theory for scattering electrons [1]. The black domain was helpful for finding a location of the platinum surface against bubbles, flaws or alumina of polish on the glass surface. Coordinate points of the boundary of the

the gray spot were read on each SEM image. They were analyzed with the least-square method for a circle to yield a radius. The radii varied slightly with magnification and accelerating voltage of the SEM. We obtained several values of radii for one electrode, and took average.

Figure 5 shows the logarithmic variation of a_{cv} with a_{sem} , together with errors (standard deviations) of a_{sem} . It also shows the line of $a_{cv} = a_{sem}$. Values of a_{cv} were the same as those of a_{sem} for diameters more than 10 μm . When diameters were smaller than 4 μm , we obtained $a_{cv} < a_{sem}$. For the smallest electrode, $2a_{sem} = 0.11 \mu\text{m}$, we evaluated only the 6 % diameter ($2a_{cv} = 0.007 \mu\text{m}$) from the current. The variation in Fig. 5 presents a problem of using the method of determining diameters less than 4 μm by Saito's equation.

As the electrode becomes small, the geometry of the surface deviated from a circle, as can be seen by the error bars in Fig. 5. The diffusion-controlled current at an elliptic electrode is very close to that at a disk electrode of which area is the same as the elliptic electrode [12]. Therefore the errors in the radius in Fig. 5 have few effects on the current values or a_{cv} .

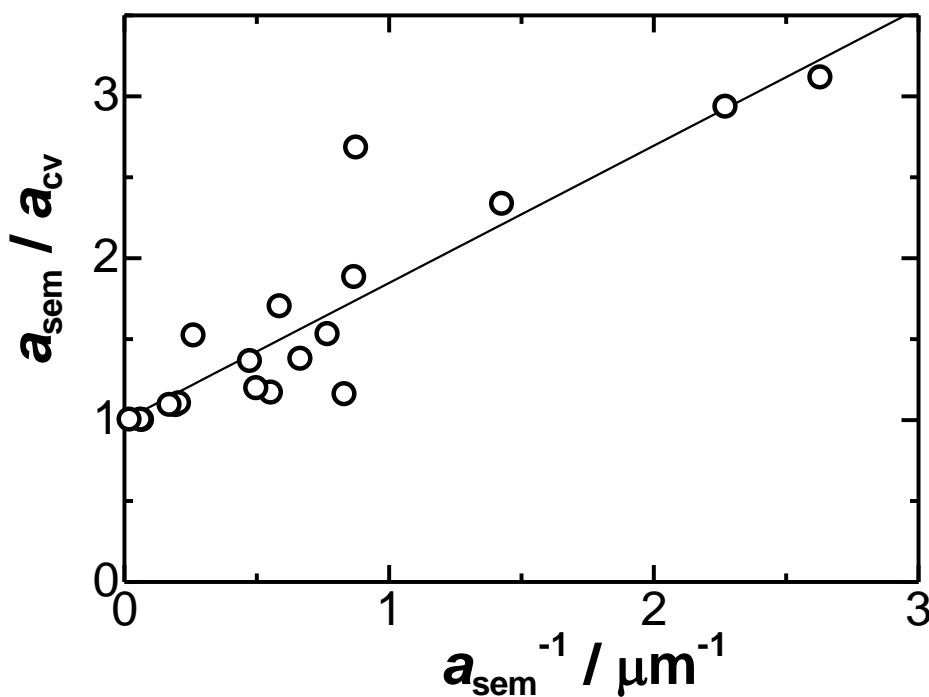


Figure 6. Variation of a_{sem}/a_{cv} with $1/a_{sem}$ on the assumption of a hemispherical electrode.

In order to analyze the relation between a_{cv} and a_{sem} in Fig. 5, we first regard the fabricated electrodes as hemispheres. By use of Eq. (9) which is valid for hemispherical electrodes, values of a_{sem}/a_{cv} are plotted against $1/a_{sem}$ for $a_{sem} > 3.3 \mu\text{m}$ in Fig. 6. Plots fell on a line with the intercept of unity. The slope gives $\delta = 0.85 \mu\text{m}$. A reason for selecting the data points to $a_{sem} > 3.3 \mu\text{m}$ is to eliminate scattering of the plot for ambiguity of a_{sem} .

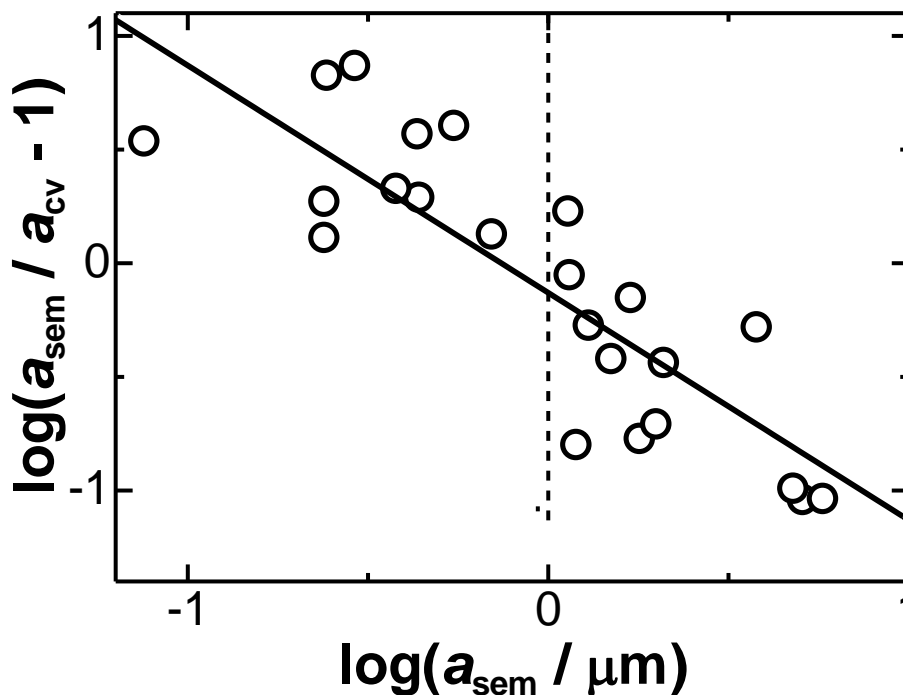


Figure 7. logarithmic plot of $a_{\text{sem}}/a_{\text{cv}} - 1$ against a_{sem} on the assumption of a disk electrode. The slope of the line is -0.952.

Another plot is of Eq. (15) for disk microelectrodes. Figure 7 shows plots of $\log(a_{\text{sem}}/a_{\text{cv}})$ against $\log(a_{\text{sem}})$. The value of the slope should be -0.952, according to Eq. (15). Although the slope by the least-square was -1.0, we drew compulsively a line with slope -0.952 by use of least-square. The intercept value gives $\delta = 0.88 \mu\text{m}$, which is close to the value (0.85) at the hemisphere model. Values of a_{cv} and a_{sem} were calculated from Eq. (16) for $\delta = 0.88 \mu\text{m}$, and are plotted in Fig. 5. They fell among the experimental values.

A question is why some researchers reported consistent values of the radii evaluated from Saito's equation with those by SEM [6-10,14,18]. Since their electrodes have been used for tips of a scanning electrochemical microscope, the electrode takes a conical or tapered form, of which side is coated with a thin film. Consequently, the steady-state currents ought to be larger than values predicted from Saito's equation, yielding values close to a_{sem} . Then, the current should be evaluated from the equation developed by Ciani and Daniele[4].

The derivation of Eq. (5) at the hemisphere and Eq. (14) at the disk electrode has been based on the delay of the flux by the displacement, δ . The delay may occur in other processes than memory diffusion, exemplified by two-dimensional diffusion on an electrode surface before the redox molecule reaches an active site, and blocking effects such as at partially coated electrodes. A key of the displacement is the potential-independence of the reaction, which can be discriminated against heterogeneous kinetics. Therefore, the deviation is observed at any potential even at the potential domain of limiting currents.

5. CONCLUSIONS

Diameters of disk-inlaid microelectrodes over 10 μm evaluated from diffusion-controlled voltammetric currents with Saito's equation are identical to the geometrical diameters. The relation, $a_{\text{cv}} < a_{\text{sem}}$, is recognized when diameters are less than 4 μm . The inequality becomes striking with a decrease in diameters. This variation is valid for a disk-exposed electrode flush on a large insulator wall. It is invalid for microelectrodes with tip type for a scanning electrochemical microscope, because the volume of the diffusion layer for the tip type is larger than the hemispherical volume. The variable relating a_{cv} with a_{sem} is the distance δ ($= 0.9 \mu\text{m}$), through which Eq. (16) satisfies the experimental data. Although Eq. (16) was derived on the basis of memory diffusion, any type of delays is conceivable.

References

1. K. Aoki, H. Takeuchi, J. Chen, T. Nishiumi, *Rev. Polarogr.* 57 (2011) 1010.
2. J.J. Watkins, J. Chen, H.S. White, H.D. Abruna, E. Maisonhaute, C. Amatore, *Anal. Chem.* 75 (2003) 3962.
3. D.-H. Woo, H. Kang, S.-M. Park, *Anal. Chem.* 75 (2003) 6732.
4. I. Ciani, S. Daniele, *Anal. Chem.* 76 (2004) 6575.
5. P. Sun, M. V. Mirkin, *Anal. Chem.* 78 (2006) 6526.
6. S. Chen, A. Kucernak, *Electrochem. Commn.* 4 (2002) 80.
7. P. Sun, M.V. Mirkin, *J. Am. Chem. Soc.* 130 (2008) 8241.
8. O. Sklyar, T.H. Treutler, N. Vlachopoulos, G. Wittstock, *Surface Sci.* 597 (2005) 181.
9. C. Wang, X. Hu, *Talanta* 68 (2006) 1322.
10. N. Gao, X. Lin, W. Jia, X. Zhang, W. Jin, *Talanta* 73 (2007) 589.
11. Y. Saito, *Rev. Polarogr. Jpn.* 15 (1968) 177.
12. K. Aoki, C. Ouyang, J. Chen, T. Nishiumi, *J. Solid State Electrochem.* 15 (2011) 2305.
13. C. Zuliani, D.A. Walsh, T.E. Keyes, R.J. Forster, *Anal. Chem.* 82 (2010) 7135.
14. I. Ciani, S. Daniele, *Anal. Chem.* 76 (2004) 6575.
15. H. Xiong, J. Guo, K. Kurihara, S. Amemiya, *Electrochem. Commn.* 6 (2004) 615.
16. J.P. Guerrette, S.M. Oja, B. Zhang, *Anal. Chem.* 84 (2012) 1609.
17. B. Zhang, Y. Zhang, H.S. White, *Anal. Chem.* 76 (2004) 6229.
18. P.J. Rodgers, S. Amemiya, *Anal. Chem.* 79 (2007) 9276.
19. J. Newman, *Electrochemical Systems*, Prentice-Hall, NJ (1973) p 344.
20. K. B. Oldham, *J. Electroanal. Chem.* 260 (1989) 461.
21. J.M. Elliott, P.R. Birkin, P.N. Bartlett, G.S. Attard, *Lagmuir* 15 (1999) 7411.
22. D. Menshykau, I. Streeter, R.G. Compton, *J. Phys. Chem. C* 112 (2008) 14428.
23. T. Gueshi, K. Tokuda, H. Matsuda, *J. Electroanal. Chem* 89 (1978) 247.
24. T. Gueshi, K. Tokuda, H. Matsuda, *J. Electroanal. Chem* 101 (1979) 29.
25. K. Tokuda, T. Gueshi, H. Matsuda, *J. Electroanal. Chem* 102 (1979) 41.
26. P. Vernotte, *Compt. rend.* 246 (1958) 3154.
27. C.E. Ulbrich, *Phys. Rev.* 123 (1961) 2001.
28. M. Chester, *Phys. Rev.* 131 (1963) 2013.
29. H. W. Load, Y. Shulman, *J. Mech. Phys. Solids*, 15 (1967) 299.
30. A. Szekeres, *Period. Polytech. Mech. Eng.* 48 (2004) 83.
31. K. Aoki, C. Xian, *J. Phys. Chem. C* 111 (2007) 15433.
32. K. Aoki, *J. Chem. Sci.* 121 (2009) 601.

33. K. Aoki, C. Zhang, J. Chen, T. Nishiumi, *Electrochim. Acta*, 55 (2010) 7328.
34. H. Zhang, K. Aoki, J. Chen, T. Nishiumi, H. Toda, E. Torita, *Electroanalysis*, 23 (2011) 947.
35. K. Aoki, *J. Electroanal. Chem.* 592 (2006) 31.
36. K. Aoki, K. Tokuda, H. Matsuda, *J. Electroanal. Chem.* 235 (1987) 87